Improving Charging Efficiency with Workload Scheduling in Energy Harvesting Embedded Systems

Yukan Zhang, Yang Ge and Qinru Qiu
Department of Electrical Engineering and Computer Science, Syracuse University
Syracuse, New York, 13244, USA
{yzhan158, yage, qiqiu}@syr.edu

ABSTRACT
In energy harvesting embedded systems, if the harvested power is sufficient for the workload, extra power will be stored in the electrical energy storage (EES) bank. How much energy can be stored is affected by many factors including the efficiency of the energy harvesting module, the input/output voltage of the DC-DC converters, the status of the EES elements, and the characteristics of the workload. This paper investigates the impact of workload scheduling of the embedded system on the storage efficiency of the EES bank. We first provide an approximated but accurate power consumption model of the DC-DC converter. Based on this model, we analytically prove that an optimal workload schedule is to always execute high power task first. Experimental results confirm that proposed scheduling strategy outperforms all other possible scheduling and increases the amount of stored energy by up to 10.41% in average.

Categories and Subject Descriptors
C.3 [**Special Purpose and Application Specific Systems**]: Real-time and embedded systems

General Terms
Algorithms, Design.

Keywords
Energy harvesting embedded system, electrical energy storage, scheduling

1. INTRODUCTION
According to a recent survey, longer battery life is more important to user satisfactory than any other features [1] for mobile embedded systems such as smartphones and tablet computers. One promising technique to extend the battery lifetime of these embedded systems is to integrate an environmental energy harvesting module as a supplement energy source. Many research works have proposed to power the embedded system directly from the harvested energy in order to reduce the battery charging and discharging overhead [2][6]. When the harvested energy is abundant, extra energy will be stored into the battery, or in a more general term, *electrical energy storage* (*EES*) element. When the harvesting rate is low, the embedded system will be powered by the EES element as usual.

The energy harvesting embedded system is a complex platform consisting of many components that work collaboratively. And the energy efficiency of the system can be improved in many aspects and at different levels of abstraction. From the perspective of embedded system optimization, the scheduling and operating frequency/voltage of the embedded processor should be carefully selected to satisfy the performance requirement as well as power/energy constraint. For example, the authors in [6] proposed an energy-harvesting aware dynamic voltage frequency selection (EA-DVFS) algorithm, which adjusts the speed of task execution based on the current energy reserve in the system. In [7], the energy savings is further improved by exploring task slacks.

From the perspective of energy harvesting optimization, the operating conditions of the harvesting modules should be set carefully to generate more power. For example, in order to draw maximum amount of power from a photovoltaic (PV) array, various maximum power point tracking (MPPT) methods [8] have been proposed that dynamically adjust the output current to match the output impedance. In a recent work [9], the authors proposed a technique to improve the PV cells' efficiency under partial shading conditions.

The DC-DC converters are also important components in the system and their energy efficiency has drawn lots of attention in recent works. In [10], the authors proposed an analytic power model for DC-DC converters and based on this model, the authors found that the overall energy consumption of the embedded application and the converter is a convex function of the processor's supply voltage. Thus the optimal operating voltage can be solved by minimizing a convex function. The DC-DC converter's power efficiency is also essential to the energy transfer between different components in the system. For example, [3][11][12] try to adjust the voltage of *charge transfer interconnect* (*CTI*) and active EES banks to reduce the power wasted on DC-DC converters. And [4] proposed to reconfigure the parallel and serial connection of the EES bank to match the input and output voltage of the DC-DC converter to reduce the DC-DC converter power consumption.

In this work, we investigate the impact of task scheduling on the efficiency of an energy harvesting embedded system. More specifically, we consider the scenario where the harvested energy is more than enough to power the embedded system and the extra power can be used to charge an EES bank. Apparently, how much power is consumed by the embedded system directly affects the amount of remaining power that goes into the EES bank. For most EES modules (e.g. supercapacitors), their terminal voltage has a monotonically increasing relation with the amount of energy stored. Different input power will increase energy storage at different rate and hence causes different terminal voltage. This affects the efficiency of the DC-DC converter, which matches the voltages between the EES and other system components. As a result, not all input energy can be stored in the EES and the efficiency of the EES charging process is affected. Our goal is to find an optimal schedule of the embedded workload such that the most energy can be stored into the EES bank.

To facilitate the development of the scheduling algorithm, we first present a simplified yet accurate approximation to model the

DAC '13, May 29 - June 07 2013, Austin, TX, USA.

power consumption of a DC-DC converter. Then we consider the most basic scheduling problem that has only two tasks with equally short execution time and different power consumptions under the scenario of fixed energy harvesting rate. Using the approximated power model, we analytically prove that, in this special scenario, executing the high power task first enables more energy to be stored in EES. We then generalize this result to multiple tasks with arbitrary lengths under general energy harvesting scenarios.

The following summarizes the technical contributions of this work:

- Although there have been many publications on battery aware task scheduling, most of them consider the non-linear property of battery when it is in discharge mode [13]. To the best of our knowledge, this is the first work that optimizes the task scheduling to increase the efficiency of EES charging process.
- Many of the existing works on EES efficiency optimization either ignore the impact of DC-DC converters ([6] and [7]) or minimize the energy waste on DC-DC using dynamic voltage selection with an assumption of fixed task scheduling [10]. This is the first work that investigates the impact of task scheduling on the energy efficiency with the consideration of the DC-DC converters.
- Our scheduling algorithm is rigorously proved to be optimal. The scheduling algorithm has very low complexity as it only has to sort the tasks based on their power consumptions.

The rest of this paper is organized as follows. The energy harvesting embedded system model and the problem definition are presented in section 2. The proposed scheduling algorithm is described in section 3. Experimental results and discussions are presented in section 4. We conclude our paper in section 5.

2. SYSTEM MODEL

In this section, we present the energy harvesting embedded system model, the DC-DC converter power consumption model and our problem definition.

2.1 Energy Harvesting Embedded System Model

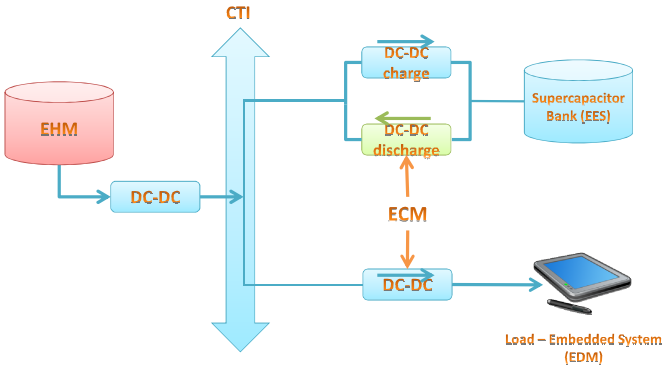

Figure 1. Energy harvesting embedded system architecture

Figure 1 shows the block diagram of the architecture of the energy harvesting embedded system considered in this paper. The system consists of the following components, an *energy harvesting module* (*EHM*), several heterogeneous *electrical energy storage* (*EES*) banks (only one bank is shown in the figure) and the embedded systems, i.e. the *energy dissipation module* (*EDM*). All these components are connected together through *Charge Transfer Interconnect* (*CTI*) and DC-DC converters. We refer those DC-DC converters as *energy conversion modules* (*ECM*). The DC-DC converters connected to EHM, EDM and ESS are called ECM_{EH}, ECM_{ED}, and ECM_{ES} respectively. The ECM_{ES} can further be divided into two function units, ECM_{ES_charge} and $ECM_{ES\_discharge}$, which involve in ESS charge and discharge processes.

Energy is harvested from the environment by EHM and distributed to other components. Any type of EHM can be integrated in our system. When the harvested power is more than sufficient for the embedded workload, the extra power will be stored in the EES bank for future use. In order to minimize the power wasted on the DC-DC converter, we assume only one EES bank is turned on at any time to accept the extra power. The efficiency of DC-DC converter increases when the difference between its input and output voltage reduces [4], by setting the voltage of the Charge Transfer Interconnect (V_{cti}) to be equal to the V_{dd} of the embedded processor, we can minimize the power wasted on ECM_{ED}. The very low V_{dd} level used by today's deep submicron technology will very likely keep V_{cti} lower than the terminal voltage of the EES bank, and consequently makes ECM_{ES} operate in the boost mode. Therefore, in this paper, we confine our discussion to the scenario where ECM_{ES} operates in boost mode.

2.2 The DC-DC Converter Power Model under Boost Mode

DC-DC converters are placed between system components and the charge transfer interconnect for voltage and current regulation. In this paper, we assume that the converters are uni-directional switching buck-boost converters as shown in Figure 2 ([4]). When the input voltage V_{in} is greater than the output voltage V_{out}, the DC-DC converter operates at buck mode. Otherwise the DC-DC converter operates at boost mode. The power consumption P_{dcdc} of the DC-DC converter strongly depends on V_{in}, V_{out} and the output current I_{out}. It consists of three components: conduction loss P_{cdct}, switching loss P_{sw} and controller loss P_{ctrl}.

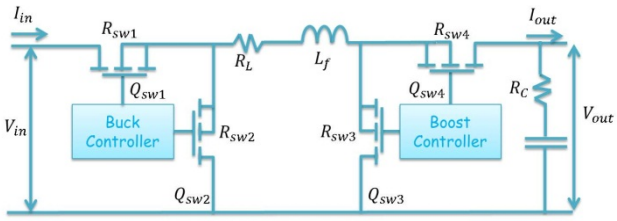

Figure 2. Energy harvesting embedded system architecture

As mentioned earlier, we focus our discussion in the scenario where the DC-DC converter operates at boost mode. In boost mode, these three power consumption components can be expressed as the following ([3]):

$$P_{cdct} = (I_{out}^2/D^2) \cdot (R_L + (1-D) \cdot R_{sw3} + D \cdot R_{sw4} + R_{sw1} + D \cdot (1-D) \cdot R_C) + (\Delta I)^2/12 \cdot (R_L + (1-D) \cdot R_{sw3} + D \cdot R_{sw4} + R_{sw1} + D \cdot R_C)$$

$$P_{sw} = V_{out} \cdot f_s \cdot (Q_{sw3} + Q_{sw4}), P_{ctrl} = V_{in} \cdot I_{ctrl}$$

where $D = V_{in}/V_{out}$ is the duty ratio and $\Delta I = V_{out} \cdot (1-D)/(L_f \cdot f_s)$ is the maximum current ripple. f_s is the switching frequency; I_{ctrl} is the current flowing into the controller; R_L and R_C are the equivalent series resistance (ESR) of inductor L and capacitor C, respectively; $R_{sw1\ldots4}$ and $Q_{sw1\ldots4}$ are the turn-on

resistances and gate charges of the four switches in Figure 2 respectively. As we could see from the above equations, P_{dcdc} is a complex non-linear function of V_{in}, V_{out} and I_{out}. To facilitate the development of an efficient task scheduling algorithm, it is desirable to derive a simple yet accurate approximation to model power consumption of the DC-DC converter. We first divide the P_{cdct} to two parts:

$$P_{cdct1} = \frac{I_{out}^2}{D^2} \cdot (R_L + (1-D) \cdot R_{sw3} + D \cdot R_{sw4} + R_{sw1} + D \cdot (1-D) \cdot R_C)$$

$$P_{cdct2} = \frac{(\Delta I)^2}{12} \cdot (R_L + (1-D) \cdot R_{sw3} + D \cdot R_{sw4} + R_{sw1} + D \cdot R_C)$$

It has been shown in [5] that the resistance R_{sw3} and R_{sw4} have about the same value, so the above equations can be reduced to

$$P_{cdct1} = \frac{I_{out}^2}{D^2} \cdot (R_L + R_{sw4} + R_{sw1} + D \cdot (1-D) \cdot R_C)$$

$$P_{cdct2} = \frac{(\Delta I)^2}{12} \cdot (R_L + R_{sw4} + R_{sw1} + D \cdot R_C)$$

Because the DC-DC converter operates at boost mode, the possible region of V_{out} is $[V_{in}, +\infty)$. When $V_{in} = V_{out}$, $P_{cdct2} = 0$; when $V_{out} \to +\infty$, $P_{cdct1} \to +\infty$ and P_{cdct2} is a finite number. In both cases, P_{cdct2} is negligible compare to P_{cdct1}. Therefore, we eliminate P_{cdct2} in the approximation model. Furthermore, because $D = 1$ when $V_{in} = V_{out}$ and $D = 0$ when $V_{out} = +\infty$, we also drop the term $D(1-D) \cdot R_c$ in the approximation model since its value is below $0.25R_C$ which is much smaller than the other terms in the function. The final approximation model is as following:

$$P_{dcdc} = P_{cdct1} + P_{sw} + P_{ctrl} = \left(\frac{I_{out}V_{out}}{V_{in}}\right)^2 \cdot (R_L + R_{sw4} + R_{sw1}) + V_{out} \cdot f_s \cdot (Q_{sw3} + Q_{sw4}) + V_{in} \cdot I_{ctrl}$$

To validate our approximation model, we fix the V_{out} at 5V and vary V_{in} from 1V to 5V and show the actual power consumption and the approximated power consumption of DC-DC converter in Figure 3. The red, blue and green lines are for $I_{out} = 1A$, $2A$ and $3A$ respectively. We can see in the figure that the approximation model closely tracks the original model.

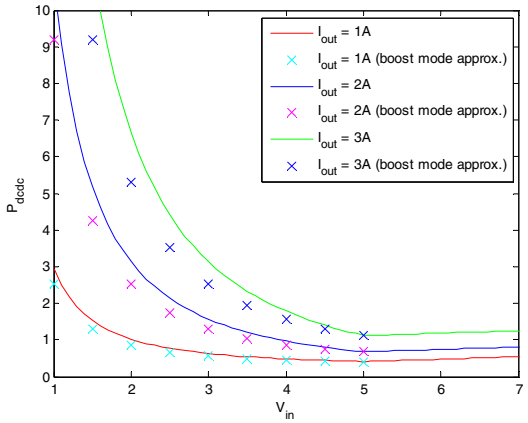

Figure 3. Approximation power model under boost mode

2.3 Problem Definition

We define our scheduling problem as following. Given an energy harvesting embedded system, which is used to process n periodic tasks $T_1, T_2, \ldots, T_n$. The set of tasks are immediately available at the beginning of a new period. Their durations are $t_1, t_2, \ldots, t_n$. Tasks are independent, non-preemptive, and the processor works in single task mode. The power consumption of task T_i is denoted as P_i. In this work, we do not consider dynamic voltage and frequency scaling of the embedded processor; therefore, the power consumption of a task is assumed to be fixed during the runtime. We assume that the energy harvesting rate is higher than the power consumption of the EDM, therefore the EES bank works in charge mode. As we explained in section 2.1, the DC-DC converter (ECM_{ES}) connecting the EES to the CTI operates in boost mode. Our goal is to find the optimal task schedule such that by the time when all tasks are completed the most energy can be stored into the EES bank.

3. Task Scheduling for Efficient EES Charging

We refer to the different charging characteristics as *charging phases* of the EES bank. When the harvesting rate is given, the identification of charging phases is solely determined by task execution. Given a set of tasks and an energy harvesting rate, executing the task with higher power consumption is equivalent to charging the EES bank using a lower input power, and vice versa. Therefore, the task scheduling can also be viewed as charge phase scheduling. In this work, we use the name *highest power workload first* (*HPWF*) to refer to the scheme that gives the top priority to execute the workload with the highest power consumption, and use the name *lowest power workload first* (*LPWF*) to refer to the scheme that gives the top priority to execute the workload with the lowest power consumption. We also use names *highest power charge first* (*HPCF*) and *lowest power charge first* (*LPCF*) to refer to the scheduling scheme that generates a sequence of EES charging phases whose input power follows descending or ascending order respectively. It is obvious that when the harvesting rate is fixed, LPWF is equivalent to HPCF and HPWF is equivalent to LPCF.

In this section, we first discuss the optimal charging phase scheduling and show that LPCF is superior to HPCF. This is proved first with the assumption that there are only two charging phases and both have the same durations that are extremely short. Then we extend this conclusion to scenarios with multiple charging phases that are equally short. Finally, we remove all constraint and generalize this conclusion to multiple charging phases with arbitrary duration. Based on this result, we further prove that HPWF is superior to LPWF.

3.1 Scheduling of Two Charging Phases with Very Short Duration

In this subsection, we consider two extremely short charging phases τ_1 and τ_2 with duration $\Delta t \to 0$, and their charging powers has the relation $P_{lo} < P_{hi}$. We denote the initial energy and voltage of the bank as (E_0, V_0). With the LPCF scheme, the bank is charged with P_{lo} in the first phase and then charged with P_{hi} in the second phase. The stored energy and voltage of the bank at the end of phase 1 and phase 2 are denoted as (E_1^{LPCF}, V_1^{LPCF}) and (E_2^{LPCF}, V_2^{LPCF}) respectively. Similarly, with the HPCF scheme, the bank is charged with P_2 in the first phase and then is charged with P_1 in the second phase. The bank energy and voltage at the end of phase 1 and phase 2 are denoted as (E_1^{HPCF}, V_1^{HPCF}) and (E_2^{HPCF}, V_2^{HPCF}) respectively.

Lemma 1. Given an EES with initial energy E_0 and initial voltage V_0. Charge this EES using two charging phases that has equal duration Δt that is extremely small. Denote the charging powers in the first and second phases as P_A and P_B respectively, and the

bank voltage at the end of first and second phases as V_A and V_B respectively. At the end of second phase, the amount of energy stored in EES is:

$$E_B = E_0 + \frac{\sqrt{\Delta(P_A,V_0)}-V_{in}^2}{2\alpha}\Delta t + \frac{\sqrt{\Delta(P_B,V_A)}-V_{in}^2}{2\alpha}\Delta t,$$

where $\Delta(P,V) = V^4 + 4\alpha(P - \beta V - \gamma V)V^2$, and α, β, and γ are positive constant parameters for the given DC-DC converter.

Proof: Based on the DC-DC power approximation model, when in boost mode, P_{dcdc} can be written as

$$P_{dcdc} = \alpha\left(\frac{P_{out}}{V_{in}}\right)^2 + \beta V_{in} + \gamma V_{out} \quad (1)$$

Substitute P_{dcdc} with $P_{in} - P_{out}$ in the above equation and rearrange the equation, we obtain

$$\alpha P_{out}^2 + V_{in}^2 P_{out} + (\beta V_{in} + \gamma V_{out} - P_{in})V_{in}^2 = 0 \quad (2)$$

Although P_{out} can have two solutions, because $P_{out} > 0$, the only valid solution is

$$P_{out} = \frac{\left(\sqrt{V_{in}^4 + 4\alpha(P_{in} - \beta V_{in} - \gamma V_{out})V_{in}^2} - V_{in}^2\right)}{2\alpha} \quad (3)$$

Based on the definition of $\Delta(P,V)$, we have

$$P_{out} = \frac{\sqrt{\Delta(P_{in},V_{out})} - V_{in}^2}{2\alpha}$$

The initial state of the bank is (E_0, V_0). After being charged using P_A for Δt, the state of the bank becomes (E_A, V_A). Because Δt is very small, we assume the output voltage of the DC-DC converter is the same during this period. Also because P_{in} and V_{in} are constant values during the same charging phase, the output power is also a constant value and is denoted as $P_{out}(P_A, V_0)$. Then we have

$$E_A = E_0 + P_{out}(P_A,V_0)\cdot\Delta t = E_0 + \frac{\sqrt{\Delta(P_A,V_0)} - V_{in}^2}{2\alpha}\Delta t \quad (4)$$

For the same reason, in the second charging phase, we charge the bank using P_B for Δt and we have

$$E_B = E_A + P_{out}(P_B,V_A)\cdot\Delta t = E_A + \frac{\sqrt{\Delta(P_B,V_A)} - V_{in}^2}{2\alpha}\Delta t$$

$$= E_0 + \frac{\sqrt{\Delta(P_A,V_0)}-V_{in}^2}{2\alpha}\Delta t + \frac{\sqrt{\Delta(P_B,V_A)}-V_{in}^2}{2\alpha}\Delta t \quad \square$$

Based on Lemma 1, we have the following theorem. The proof of the theorem is provided in the supplemental section.

Theorem 1. Given that both charging phases have equal durations which are approaching to 0, the system follows LPCF scheme has more stored energy at the end of phase 2 than the system follows HPCF scheme, i.e. $E_2^{LPCF} > E_2^{HPCF}$.

3.2 Scheduling of Multiple Charging Phases with Equally Short Durations

In this subsection, we consider the scheduling problem for arbitrary number of extremely short charging phases $\tau_1, \tau_2, \dots, \tau_n$ with duration $\Delta t \to 0$, and their charging powers are $P_1, \dots, P_n$. Before giving the theorem, we first give a lemma.

Lemma 2. Given two identical EES bank B_1 and B_2 with initial energy $E_1 < E_2$. After charging them using the same power P for the same duration T, the energy in B_1 is less than or equal to the energy in B_2, i.e. $E_1' \le E_2'$.

Proof: Assume it takes time t to charge B_1 from E_1 to E_2 using P. Then after time $T - t$, bank B_2 reaches E_1', which equals the final energy of B_1 after time T. Continue to charge B_2 for time t, we have $E_2' \ge E_1'$.

Theorem 2. Given n charging phases $\tau_1, \tau_2, \dots, \tau_n$, with duration $\Delta t \to 0$, scheduling them based on the ascending order of their power maximizes the amount of energy stored in EES. Such scheduling policy is referred as LPCF (i.e. Lowest Power charging First).

Proof: We will prove this theorem using induction and contradiction. We know from Theorem 1 that the statement is true when $n = 2$. Assume LPCF scheme is the optimal scheduling policy for any i charging phases as long as $i \le N$, we are going to prove LPCF scheme is the best for $N + 1$ charging phases.

Assume the energy optimal scheduling for the $N + 1$ charging phases are $S_{opt} = \{\tau_1, \tau_2, \dots, \tau_{N+1}\}$, and their power are not in the ascending order. This means that there are two tasks τ_i and τ_{i+1} such that $P_i > P_{i+1}$. Then we construct a new schedule by switching phases τ_i and τ_{i+1} and get $S' = \{\tau_1, \dots, \tau_{i+1}, \tau_i, \dots, \tau_{N+1}\}$. Note that after charging phase τ_{i-1}, the energy stored by both S_{opt} and S' are the same, because the first $i - 1$ charging phases are the same for the two schedules. For the next two charging phases, schedule $\{\tau_i, \tau_{i+1}\}$ is worse than schedule $\{\tau_{i+1}, \tau_i\}$ because $P_{i+1} < P_i$. Therefore, at the end of $(i + 1)$th charging phase, schedule S' stores more energy than the schedule S_{opt}. Because the remaining $N - i - 1$ charging phases are the same for both schedules, based on Lemma 2, S' stores more energy than S_{opt} at the end of all charging phases. This contradicts the assumption that S_{opt} is the energy optimal scheduling. Therefore, for $N + 1$ charging phases, the optimal scheduling is still the LPCF scheme.

From the above discussions, we have seen that for arbitrary number of very short charging phases, the LPCF scheme is the most energy efficient scheduling.

3.3 Scheduling of Arbitrary Charging Phases

In this subsection, we consider the scheduling problem for multiple charging phases with arbitrary duration. We claim that the LPCF scheme is still the best scheduling. This can be proved by dividing charging phases into very small slices such that $t_i = N_i \Delta t$, where t_i is the duration of the ith charging phase. We consider each slice as a sub-phase. All sub-phases belonging to the ith phase have the same charging power P_i.

Based on the discussion of previous sections, to reach the highest energy efficiency, these sub-phases should be arranged based on LPCF scheme. All sub-phases having the lowest charging power will be scheduled first, followed by the sub-phases having the second lowest charging power. This is equivalent as scheduling the charging phases from low power to high power, in another word, to execute tasks with highest power consumptions first.

3.4 Task Scheduling to Improve Charging Efficiency

It is easy to know that when the energy harvest rate is fixed, task scheduling and charging phase scheduling have direct correspondence. HPWF is the optimal task scheduling because it leads to LPCF, which has been proved to be optimal in previous sections. In the next we will show that HPWF is the optimal even if the energy harvesting rate is time varying.

We first consider the case when the harvesting power is monotonically increasing or decreasing. When the harvesting power is monotonically increasing, the highest power workload

first (HPWF) scheduling will produce a sequence of charging phases with monotonically increasing input power. So it is equivalent to the LPCF, which is optimal as proved.

In the next, we will show that the HPWF scheduling is still optimal when the harvesting rate is monotonically decreasing. Similar to section 3.1, we first consider two very short tasks t_{hi} and t_{lo}, with duration $\tau \to 0$ and power consumption R_{hi} and R_{lo}. Without loss of generality, we assume $R_{hi} > R_{lo}$. The harvesting power during time period $[0,\ \tau]$ and $[\tau,\ 2\tau]$ is denoted as Q_1 and Q_2 respectively. We assume harvesting power is more than enough to power either one of the two tasks, i.e. $\min(Q_1, Q_2) > \max(R_{hi}, R_{lo})$. We focus our discussion to the case where the harvesting energy is decreasing, i.e. $Q_1 > Q_2$.

Based on the relations between $R_{hi},\ R_{lo}$ and Q_1, Q_2, we have two possible cases:

Case1: $Q_1 - R_{hi} > Q_2 - R_{lo}, Q_1 - R_{lo} > Q_2 - R_{hi}$.

Case 2: $Q_1 - R_{hi} < Q_2 - R_{lo}, Q_1 - R_{lo} > Q_2 - R_{hi}$.

We denote $P_1 = Q_1 - R_{hi},\ P_2 = Q_2 - R_{lo}$ and $P_1' = Q_1 - R_{lo},\ P_2' = Q_2 - R_{hi}$. It is easy to see that if we execute task t_{hi} during the period $[0,\ \tau]$ and task t_{lo} during the period $[\tau, 2\tau]$, we are also charging the EES with input power P_1 during the period $[0,\ \tau]$ and input power P_2 during the period $[\tau, 2\tau]$. On the other hand, if we execute t_{lo} followed by task t_{hi}, we are charging the EES with P_1' for the duration $[0,\ \tau]$ and P_2' for the duration $[\tau, 2\tau]$. Furthermore, $P_1 + P_2 = P_1' + P_2' = P$.

We will first prove that, under case 1, HPWF is better than LPWF, i.e. charging EES with (P_1, P_2) is better than charging with (P_1', P_2').

Based on the lemma 1, using HPWF, the final energy stored in EES bank can be calculated as:

$$E_2 = E_0 + \frac{\sqrt{\Delta(P_1, V_0) - V_{in}^2}}{2\alpha}\Delta t + \frac{\sqrt{\Delta(P_2, V_1) - V_{in}^2}}{2\alpha}\Delta t$$

We are interested in finding the derivative of E_1' against P_1, i.e. dE_1'/dP_1. Based on the definition of $\Delta(P_1, V_0)$ and given that $P_2 = P - P_1$, and E_0, V_{in} do not depend on P_1, the derivative is:

$$\frac{dE_1'}{dP_1} = \frac{1}{\sqrt{\Delta(P_1, V_0)}}\Delta t - \frac{1 + \frac{\gamma}{CV_0\sqrt{\Delta(P_1, V_0)}}}{\sqrt{\Delta(P_2, V_1)}}\Delta t$$

Based on the definition of $\sqrt{\Delta(P_1, V_0)}$, we have $\sqrt{\Delta(P_1, V_0)} > \sqrt{\Delta(P_2, V_1)}$ because $P_1 > P_2$. Since $\gamma > 0$, we also have $1 + \frac{\gamma}{CV_0\sqrt{\Delta(P_1, V_0)}} > 1$. Together, we have $dE_1'/dP_1 < 0$, when $P_1 > P_2$. This means E_1' is a decreasing function against P_1, if $P_1 > P_2$. Because $P_1' > P_1$, charging with (P_1, P_2) is better than charging with (P_1', P_2'). So for case 1, HPWF is better than LPWF.

For case 2, we note that, first, charging with (P_1, P_2) is better than $(P_2,\ P_1)$, because (P_1, P_2) is LPCF. Then based on the discussion for case 1, we know $(P_2,\ P_1)$ is better than (P_1', P_2'), because $P_2 < P_1'$. Therefore HPWF is still better for case 2.

We have proved that HPWF scheduling is optimal for two very short tasks under monotonically decreasing harvesting power. This result can be extended to any number of tasks with arbitrary duration by using the same techniques in section 3.2 and 3.3.

Because HPWF is the optimal scheduling policy for scenarios with either monotonously increasing or decreasing energy harvesting rate, we can conclude that no matter how the harvesting changes, the HPWF scheduling scheme could always store the most energy into the EES banks.

4. EXPERIMENTAL RESULTS

To demonstrate the effectiveness of the proposed algorithm, we implement a C++ simulator to model the energy harvesting embedded system. We assume the system has one customized supercapacitor [14] with 40F capacitance and 15V rated voltage as the EES element. This configuration is similar to the one provided in [15]. We obtain the parameters of the DC-DC power converter model from [5]. These parameters are obtained from the datasheets of the real devices. We also assume the V_{dd} of the embedded system is 1.0V and the V_{cti} is also operated at 1.0V to match V_{dd}. The initial bank terminal voltage is also set to 1.0V.

4.1 Scheduling for Two Charging Phases

In the first set of experiments, we examine the impact of the scheduling for two charging phases with different charging power. Because there are only two charging phases, only two possible schedules are available: the LPCF and the HPCF scheme.

We first set the input power of one charging phase to be 0.5W and sweep the other from 0.2W to 1.0W. Note that the input power here is the extra harvested power after supplying the embedded system. We skip the case when both charging phases are 0.5W. We also set the duration of both charging phases to be 30 min. This duration is similar to the military radio application [11]. Table 1 Shows the energy stored in the EES element for the two scheduling schemes. As we can see, the LPCF scheme always performs better than the HPCF scheme as expected, and the difference could be up to 24.6%.

Table 1 Comparison of energy stored by HPCF &LPCF

Power (W)	0.2	0.3	0.4	0.6	0.7	0.8	0.9	1.0
HPCF (J)	419.9	419.9	495.8	711.4	789.5	868.3	946.8	1069.2
LPCF (J)	442.9	496.9	562.5	773.3	910.5	1046.2	1179.9	1311.4
Impr. (%)	5.46%	18.34%	13.45%	8.70%	15.33%	20.49%	24.61%	22.65%

As the input power increases in one of the charging phases and remains fixed in the other, the total energy stored in the EES element generally increases for both HPCF and LPCF. However, we also note that for the HPCF scheme, when the incoming power in one of the charging phase changes from 0.2W to 0.3W, the stored energy remains the same and all input power is consumed by the DC-DC converter. In fact, there is a minimum input power that is required to charge the EES bank. It can be estimated by setting $P_{in} = P_{dcdc}$ and $P_{out} = 0$ in our approximation model given by Equation (1). The minimum required input power is a function of V_{in} and V_{out}:

$$P_{in} = \beta V_{in} + \gamma V_{out}$$

which means we need more input power in order to break even of the consumption in the DC-DC converter when the terminal voltage of EES bank (i.e. V_{out}) increases. This can be viewed as an intuitive explanation of why LPCF is always better than the HPCF scheme. With the HPCF scheme, high power charging phase will first raise the terminal voltage of the EES bank to a high level, which reduces the opportunity for the bank to be charged in the future.

In the next experiment, we sweep the charging power from 0.2W to 1.0W with a step of 0.1W for both phases. The duration of each phase is still kept at 30 min. Figure 4 shows the improvement of LPCF over HPCF for all possible combinations of charging phases. We could see that LPCF performs better than HPCF in all cases. And the average improvement is 10.41%. When the duration of the charge phase is set to 20min and 10min, the average improvement is 9.14% and 6.86% respectively.

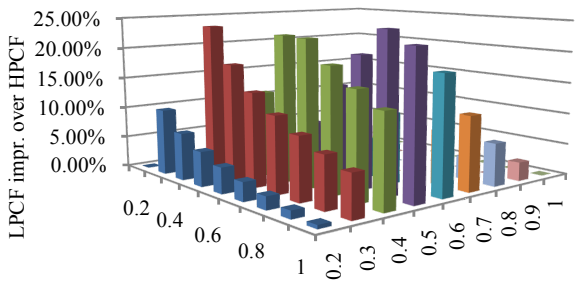

Figure 4. Improvement of LPCF over HPCF when sweep power from 0.2w to 1w

4.2 Scheduling Results for Multiple Tasks

In the second set of experiments, we examined the impact of task scheduling for multiple tasks on the energy stored in the EES bank. Various system configurations are tested. The number of tasks in each configurations are set to 6, 8 and 10; the task durations varies from 100s, 300s to 600s; and the harvesting power varies from 1.2W, 1.4W to 1.6W. The power consumption of each task is uniformly distributed between [0.2W, 1.0W]. We compare our LPCF scheme with HPCF scheme and the average results of 400 random generated schedules.

Table 2. HPCF, LPCF and Random for Multiple Tasks

		1.2 W			1.4 W			1.6 W		
	Sec	100	300	600	100	300	600	100	300	600
8 tasks	HPCF (J)	384.3	835.1	1364.5	514.4	1174.0	1935.4	644.2	1545.0	2600.1
	LPCF (J)	405.7	939.6	1598.6	535.7	1294.2	2238.7	663.6	1652.1	2901.3
	avg (J)	393.3	879.6	1458.4	524.0	1227.7	2065.1	653.0	1593.3	2735.6
	Im. H	5.58%	12.5%	17.2%	4.15%	10.2%	15.7%	3.01%	6.94%	11.6%
	Im. A	3.15%	6.83%	9.61%	2.23%	5.42%	8.41%	1.62%	3.69%	6.06%
6 tasks	HPCF (J)	389.3	807.1	1262.8	488.5	1086.9	1783.2	585.4	1364.1	2307.4
	LPCF (J)	400.2	873.0	1450.9	498.4	1145.4	1951.3	594.6	1417.1	2459.4
	avg (J)	394.7	839.0	1354.4	493.4	1115.4	1865.1	589.9	1390.0	2381.8
	Im. H	2.81%	8.17%	14.9%	2.03%	5.39%	9.43%	1.56%	3.89%	6.59%
	Im. A	1.42%	4.05%	7.12%	1.03%	2.69%	4.62%	0.79%	1.95%	3.26%
10 tasks	HPCF (J)	493.8	1154.6	1921.9	656.7	1592.5	2677.4	816.4	2049.8	3536.0
	LPCF (J)	519.8	1275.2	2208.9	679.9	1716.3	3012.5	837.6	2160.9	3840.4
	avg (J)	507.3	1215.3	2065.4	668.8	1657.0	2852.5	827.5	2107.9	3696.8
	Im. H	5.27%	10.5%	14.9%	3.53%	7.78%	12.5%	2.59%	5.42%	8.61%
	Im. A	2.47%	4.93%	6.94%	1.66%	3.58%	5.61%	1.22%	2.51%	3.88%

Table 2 reports the amount of stored energy for EES under LPCF, HPCF and the average random scheduling for all test cases. It also reports the relative improvement of LPCF over HPCF and random scheduling. We could see from this table that the LPCF scheme consistently outperforms the HPCF as well as the random scheduling policy in all test cases. And the improvement can be up to 17.15% over the HPCF scheme and 9.61% over the random scheduling. The HPCF always stores the least energy, which is even less than the worst cases in the random schedules. We observe that in some settings where the phase duration is short, the terminal voltage of the EES bank stays relatively low all the time. These cases are in general less sensitive to the scheduling order, so the difference between the three scheduling schemes is small. This explains the trend that the results for cases with 600s phase duration are generally better than the cases with 100s phase duration. For the similar reason, when the harvesting power increases, the system becomes less sensitive to the charging phase order. On the other hand, some settings are more sensitive to the scheduling. For example when the harvesting power is 1.2W and duration is 600s. In these cases, inappropriately charging the EES bank with high power first will raise the terminal voltage of EES bank and prevent it to be further charged at low power phase.

5. CONCLUSIONS

In this paper, we investigate the effects of workload scheduling on the efficiency of the EES charge process in an energy harvesting embedded system. We found that low power first scheme always performs better than the high power first scheme. It is proved using an approximated but accurate power model of the DC-DC converter. Experimental results show that the LPCF outperforms the HPCF by up to 10.41% for two charging phases. For multiple tasks, LPCF outperforms HPCF by up to17.15% and outperforms the random scheduling scheme by up to 9.61%.

6. REFERENCES

[1] K. Kumar, Y. Lu, "Cloud Computing for Mobile Users: Can Offloading Computation Save Energy?," in *IEEE Computer*, Apr. 2010.

[2] C. Moser, L. Thiele, D. Brunelli and L. Benini, "Adaptive Power Management in Energy Harvesting Systems," in *Proc. Design, Automation & Test in Europe Conference*, Apr. 2007.

[3] Q. Xie, Y. Wang, Y. Kim, N. Chang and M. Pedram, "Charge allocation for hybrid electrical energy storage systems," in *Proc. of the International Conference on Hardware/Software Codesign and System Synthesis,* Oct. 2011.

[4] Y. Kim, S. Park, Y. Wang, Q. Xie, N. Chang, M. Poncino, and M. Pedram, "Balanced reconfiguration of storage banks in a hybrid electrical energy storage system," in *Proc. of Int'l Conference on Computer Aided Design,* Nov. 2011.

[5] D. Shin, Y. Wang, N. Chang, and M. Pedram, "Battery-supercapacitor hybrid system for high-rate pulsed load applications," in *Proc. of Design Automation and Test in Europe,* Mar. 2011.

[6] S. Liu, Q. Qiu, Q. Wu, "Energy Aware Dynamic Voltage andFrequency Selection for Real-Time Systems with Energy Harvesting", in *Proc. of Design Automation and Test in Europe*, Mar. 2008.

[7] S. Liu, Q. Wu and Qinru Qiu, "An Adaptive Scheduling and Voltage/Frequency SelectionAlgorithm for Real-time Energy Harvesting Systems", in *Proc. Of Design Automation Conference*, Jul. 2009.

[8] D. Hohm and M. Ropp, "Comparative study of maximum power point tracking algorithms using an experimental, programmable, maximum power point tracking test bed," in *IEEE PSC*, 2000.

[9] X. Lin, Y. Wang, S. Yue, D. Shin, N. Chang and M. Pedram, "Near-optimal, dynamic module reconfiguration in a photovoltaic system to combat partial shading effects." in *Proc. of Design Automation Conference*, Jun. 2012.

[10] Y. Choi, N. Chang and T. Kim, "DC–DC Converter-Aware Power Management for Low-Power Embedded Systems," in *IEEE Trans. Computer-Aided Design of Integrated Circuits and Systems*, vol.26, no.8, Aug. 2007.

[11] Q. Xie, Y. Wang, M. Pedram, Y. Kim, D. Shin and N. Chang, "Charge replacement in hybrid electrical energy storage systems," in *Proc. of Asia and South Pacific Design Automation Conference,* Jan. 2012.

[12] Y. Wang, Y. Kim, Q. Xie, N. Chang, and M. Pedram, "Charge migration efficiency optimization in hybrid electrical energy storage (HEES) systems," in *Proc. of Int'l Symp. Low Power Electronics and Design,* Aug. 2011.

[13] P. Stanley-Marbell and D. Marculescu, "Dynamic fault-tolerance and metrics for battery powered, failure-prone systems," in *Proc. of Int'l Conference on Computer Aided Design,* Nov. 2003.

[14] http://www.tecategroup.com/ultracapacitors-supercapacitors/custom-modules.php

[15] http://www.tecategroup.com/capacitors/datasheets/powerburst/PBD.pdf

7. SUPPLEMENTAL MATERIAL

7.1 Proof of Theorem 1

Theorem 1. Given that both charging phases have equal durations which are approaching to 0, the LPCF scheme gives more stored energy than the HPCF scheme, i.e. $E_2^{LPCF} > E_2^{HPCF}$.

Proof:

For the LPCF scheme, we charge the bank using P_{lo} followed by P_{hi}. Both charging phases lasts for Δt. Based on Lemma 1 the final energy stored in the EES is:

$$E_2^{LPCF} = E_1 + P_{out}(P_{hi}, V_1^{LPCF}) \cdot \Delta t = E_1 + \frac{\sqrt{\Delta(P_{hi}, V_1^{LPCF})} - V_{in}^2}{2\alpha}\Delta t$$

$$= E_0 + \frac{\sqrt{\Delta(P_{lo}, V_0)} - V_{in}^2}{2\alpha}\Delta t + \frac{\sqrt{\Delta(P_{hi}, V_1^{LPCF})} - V_{in}^2}{2\alpha}\Delta t$$

,where V_1^{LPCF} is the bank voltage at the end of phase 1 for the system using LPCF scheme.

Similarity, with the HPCF scheme, the final energy in EES is:

$$E_2^{HPCF} = E_0 + \frac{\sqrt{\Delta(P_{hi}, V_0)} - V_{in}^2}{2\alpha}\Delta t + \frac{\sqrt{\Delta(P_{lo}, V_1^{HPCF})} - V_{in}^2}{2\alpha}\Delta t$$

After eliminating the common terms we can see that, in order to prove $E_2^{LPCF} > E_2^{HPCF}$, we only need to prove the following inequality:

$$\sqrt{\Delta(P_{lo}, V_0)} + \sqrt{\Delta(P_{hi}, V_1^{LPCF})} > \sqrt{\Delta(P_{hi}, V_0)} + \sqrt{\Delta(P_{lo}, V_1^{HPCF})} \quad (5)$$

Before proving (5), let us first find the relation between V_0 and V_1^{LPCF} or V_1^{HPCF}. For simplicity, we use supercapacitor as the EES bank in our proof. (The same discussion can be applied to any EES bank as long as its terminal voltage is a monotonically increasing function of its energy.)

Let P denote the input power, V_0 and V_1 denote the initial bank voltage and the bank voltage after first charging phase. The energy of a supercapacitor can be represented as $E = \frac{1}{2}CV^2$. We used this to replace E in (4), and have

$$\frac{1}{2}CV_1^2 = \frac{1}{2}CV_0^2 + \frac{\sqrt{\Delta(P\ \ , V_0)} - V_{in}^2}{2\alpha}\Delta t$$

or equivalently

$$C(V_1 - V_0)(V_1 + V_0) = \frac{\sqrt{\Delta(P\ \ , V_0)} - V_{in}^2}{\alpha}\Delta t$$

Because $\Delta t \to 0$, we could assume that $V_1 \approx V_0$, and $V_1 + V_0 \approx 2V_0$. Therefore, we have

$V_1 = V_0 + \frac{\sqrt{\Delta(P\ \ , V_0)} - V_{in}^2}{2\alpha C V_0}\Delta t$.

Therefore, we have:

$V_1^{LPCF} = V_0 + \frac{\sqrt{\Delta(P_{lo}, V_0)} - V_{in}^2}{2\alpha C V_0}\Delta t$ and $V_1^{HPCF} = V_0 + \frac{\sqrt{\Delta(P_{hi}, V_0)} - V_{in}^2}{2\alpha C V_0}\Delta t$

We expand the V_1^{LPCF} and V_1^{HPCF} in $\Delta(P_{hi}, V_1^{LPCF})$ and $\Delta(P_{lo}, V_1^{HPCF})$:

$$\Delta\left(P_{hi}, V_1^{LPCF}\right) = V_{in}^4 + 4\alpha\left(P_{hi} - \beta V_{in} - \gamma(V_0 + \frac{\sqrt{\Delta(P_{lo}, V_0)} - V_{in}^2}{2C\alpha V_0}\Delta t)\right)V_{in}^2 = \Delta(P_{hi}, V_0) - \frac{2\gamma(\sqrt{\Delta(P_{lo}, V_0)} - V_{in}^2)V_{in}^2}{CV_0}\Delta t$$

$$\Delta\left(P_{lo}, V_1^{HPCF}\right) = V_{in}^4 + 4\alpha\left(P_{lo} - \beta V_{in} - \gamma(V_0 + \frac{\sqrt{\Delta(P_{hi}, V_0)} - V_{in}^2}{2C\alpha V_0}\Delta t)\right)V_{in}^2 = \Delta(P_{lo}, V_0) - \frac{2\gamma(\sqrt{\Delta(P_{hi}, V_0)} - V_{in}^2)V_{in}^2}{CV_0}\Delta t$$

We plug the above two equations into equation (5), the left side becomes:

$$\sqrt{\Delta(P_{lo}, V_0)} + \sqrt{\Delta(P_{hi}, V_1^{LPCF})} = \sqrt{\Delta(P_{lo}, V_0)} + \sqrt{\Delta(P_{hi}, V_0) - \frac{2\gamma(\sqrt{\Delta(P_{lo}, V_0)} - V_{in}^2)V_{in}^2}{CV_0}\Delta t} \quad (6)$$

While the right side becomes:

$$\sqrt{\Delta(P_{hi}, V_0)} + \sqrt{\Delta(P_{lo}, V_1^{HPCF})} = \sqrt{\Delta(P_{hi}, V_0)} + \sqrt{\Delta(P_{lo}, V_0) - \frac{2\gamma(\sqrt{\Delta(P_{hi}, V_0)} - V_{in}^2)V_{in}^2}{CV_0}\Delta t} \quad (7)$$

Then we take square on both (6) and (7), and denote $\Delta(P, V_0)$ as $f(P)$, we have

$$f(P_{lo}) + f(P_{hi}) - \frac{2\gamma\left(\sqrt{f(P_{lo})} - V_{in}^2\right)V_{in}^2\Delta t}{CV_0} + 2\sqrt{f(P_{lo})f(P_{hi}) - \frac{2f(P_{lo})\gamma\left(\sqrt{f(P_{lo})} - V_{in}^2\right)V_{in}^2\Delta t}{CV_0}}$$

And

$$f(P_{lo}) + f(P_{hi}) - \frac{2\gamma\left(\sqrt{f(P_{hi})} - V_{in}^2\right)V_{in}^2\Delta t}{CV_0} + 2\sqrt{f(P_{lo})f(P_{hi}) - \frac{2f(P_{hi})\gamma\left(\sqrt{f(P_{hi})} - V_{in}^2\right)V_{in}^2\Delta t}{CV_0}}$$

Eliminate the common terms in the above two equations, to prove (5), it is sufficient to prove the two inequalities below

$$-\frac{2\gamma\left(\sqrt{f(P_{lo})} - V_{in}^2\right)V_{in}^2\Delta t}{CV_0} > -\frac{2\gamma\left(\sqrt{f(P_{hi})} - V_{in}^2\right)V_{in}^2\Delta t}{CV_0}$$

$$-\frac{2f(P_{lo})\gamma\left(\sqrt{f(P_{lo})} - V_{in}^2\right)V_{in}^2\Delta t}{CV_0} > -\frac{2f(P_{hi})\gamma\left(\sqrt{f(P_{hi})} - V_{in}^2\right)V_{in}^2\Delta t}{CV_0}$$

Here we need to state two properties of $f(P)$.

(1) Because $\frac{df(P)}{dP} = 4\alpha > 0$, $f(P)$ is an increasing function of P. So $f(P_{hi}) > f(P_{lo})$.

(2) Based on Equation (3), we have

$$\frac{\sqrt{f(P_{lo})} - V_{in}^2}{2\alpha} = \frac{\sqrt{\Delta(P_{lo}, V_0)} - V_{in}^2}{2\alpha} = P_{out} > 0$$

Therefore, $\sqrt{f(P_{hi})} > \sqrt{f(P_{lo})} > V_{in}^2$. And consequently

$$f(P_{lo})\left(\sqrt{f(P_{lo})} - V_{in}^2\right) < f(P_{hi})\left(\sqrt{f(P_{hi})} - V_{in}^2\right).$$

Given these two properties, it is not difficult to see that the two inequalities holds for $P_{hi} > P_{lo}$.

Combining the discussions above, we proved Theorem 1.